

STRUCTURAL STUDIES OF MATERIALS FOR HYDROGEN STORAGE

Final report - High Resolution SR-PXD measurement: 01-01-745 Beamline BM01B

Initial comment

The Physics Department at Institute for Energy Technology has a strong activity on hydrogen storage materials, involving many national and international collaborators. The strong position of the group is to a high degree owing to the good access to neutrons for powder neutron diffraction (PND) using the diffractometer PUS at the Institute's research reactor JEEP II.

Synchrotron power X-ray diffraction (SR-PXD) is an invaluable supplement to PND due to the superior speed and resolution. The data acquisition times are typically 3 orders of magnitude shorter using the MAR345 image plate at BM01A compared to PUS. This allows in-situ investigations of chemical reactions that we cannot possibly follow with PND. The very high resolution offered at BM01B allows indexing and space group determination from complex structures where the problem with peak overlapping makes the task unmanageable with PND- or laboratory PXD data.

Thus, the predictable, long-term access to the beam lines at SNBL through the long-term projects 01-01-745 and 01-02-772, has been an invaluable supplement to our neutron diffraction facilities and the rest of our experimental activity.

The crystal structures of $\text{LiMg}(\text{AlD}_4)_3$ and LiMgAlD_6

'Alanate' (AlH_4^- or AlH_6^{3-} based complex hydrides) have been extensively investigated since the discovery of reversible hydrogen desorption from Ti-enhanced NaAlH_4 .

The mixed alanes $\text{LiMg}(\text{AlH}_4)_3$ and its thermal decomposition product LiMgAlH_6 have been known since 1970, but their crystal structures have remained unknown.

Deuterated $\text{LiMg}(\text{AlD}_4)_3$ was synthesised by ball milling LiAlD_4 and MgCl_2 , yielding a mixture of poorly crystalline $\text{LiMg}(\text{AlD}_4)_3$ and LiCl . Purer (~10wt% LiCl), well-crystalline $\text{LiMg}(\text{AlD}_4)_3$ was obtained by recrystallization in diethyl ether.

High-resolution SR-PXD data were collected at BM01B and used for indexing and space group determination ($a = 8.37113(16) \text{ \AA}$, $b = 8.73910(17) \text{ \AA}$, $c = 14.3012(3) \text{ \AA}$ and $\beta = 124.8308(8)^\circ$, space group $P2_1/c$). The data were used in combination with high-resolution PND data from the PUS diffractometer at the JEEP II reactor (Kjeller, Norway) for ab-initio structure determination using the global optimization approach. The structure model was refined by according to the Rietveld method (Figure 1).

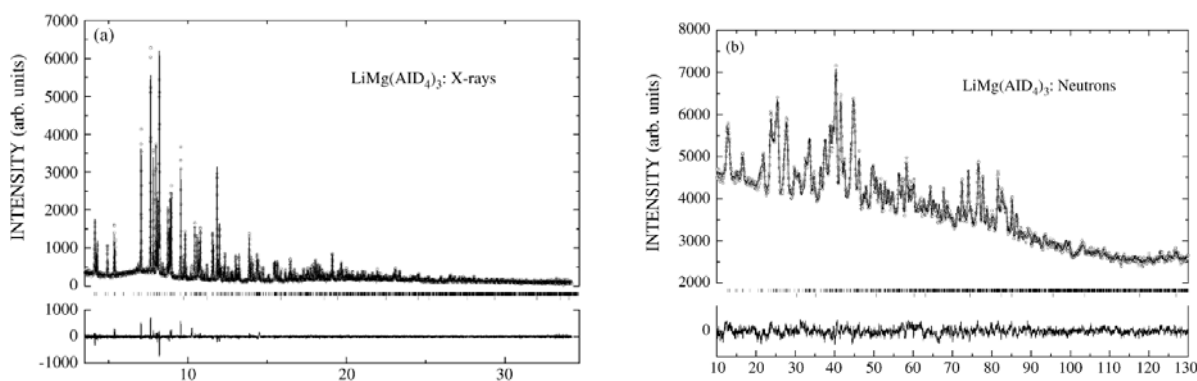


Figure 1 Rietveld fits of $\text{LiMg(AlD}_4)_3$ to a) SR-PXD data and b) PND data. Upper and lower tick marks show Bragg peaks from $\text{LiMg(AlD}_4)_3$ and LiCl , respectively.

Both Li and Mg were found to be octahedrally coordinated by D atoms from six different AlD_4 tetrahedra. Thus, the crystal structure of $\text{LiMg(AlD}_4)_3$ can be regarded as a corner-sharing network of LiD_6 and MgD_6 octahedra and AlD_4 tetrahedra. Moreover, the AlD_4 form a distorted hexagonal close-packed lattice, which thus have Li or Mg in 2/3 of the octahedral interstices. execute

A mixture of LiMgAlD_6 and Al was prepared by thermal decomposition of $\text{LiMg(AlD}_4)_3$. The product was measured by high-resolution SR-PXD (BM01B) and PND (PUS, JEEP II). A structure model was already predicted from DFT calculations (unpublished). Rietveld refinement was performed against the SR-PXD and PND simultaneously, and the DFT model was basically confirmed with minor modifications (space group $P321$ $a = 7.9856(4)$ Å $c = 4.3789(3)$ Å) (Figure 2)

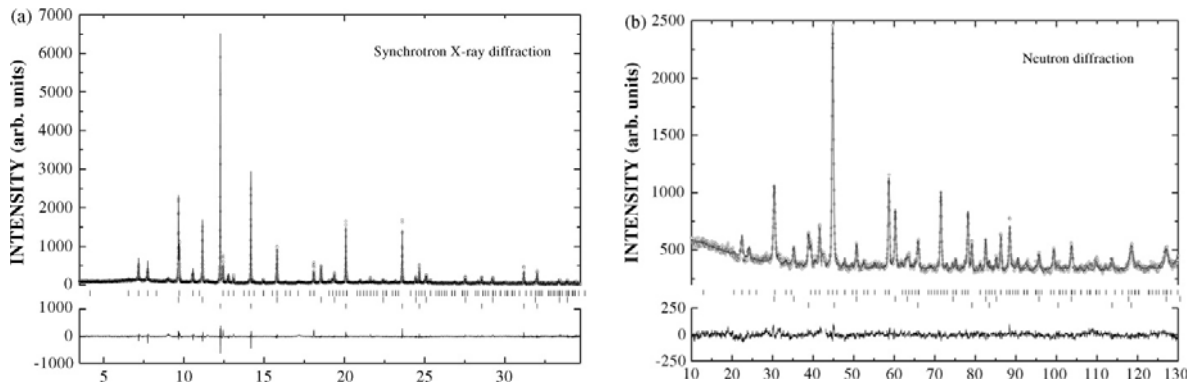


Figure 2 Rietveld fits of LiMgAlD_6 to a) SR-PXD data and b) PND data. Upper, middle and lower tick marks show Bragg peaks from LiMgAlD_6 , LiCl and Al, respectively.

The results are published in two separate papers in Journal of Alloys and Compounds [1, 2].

The crystal structure of $\text{Ca(AlD}_4)_2$

The existence of $\text{Ca(AlH}_4)_2$ has been known for some time, but it has proven difficult to synthesis the solvent-free phase by wet chemical methods. Solvent free $\text{Ca(AlD}_4)_2$ was prepared by ball milling CaD_2 and AlD_3 in the proper stoichiometric ratio.

The product was measured by high-resolution SR-PXD (BM01B) and PND (PUS, JEEP II). A structure predicted from DFT calculations was taken as the starting point for combined Rietveld refinement. The predicted orthorhombic $\text{Ca(BF}_4)_2$ -type structure was basically confirmed ($a = 13.4491(27)$ Å $b = 9.5334(19)$ Å $c = 9.0203(20)$ Å, space group $Pbca$). The

Ca atom is coordinated by 8 D from 8 different AlD_4 -ions in a square antiprismatic way. The overall structure is layered, with empty plans parallel to the bc-plane (Figure 4).

A manuscript is submitted to Journal of Alloys and Compounds.

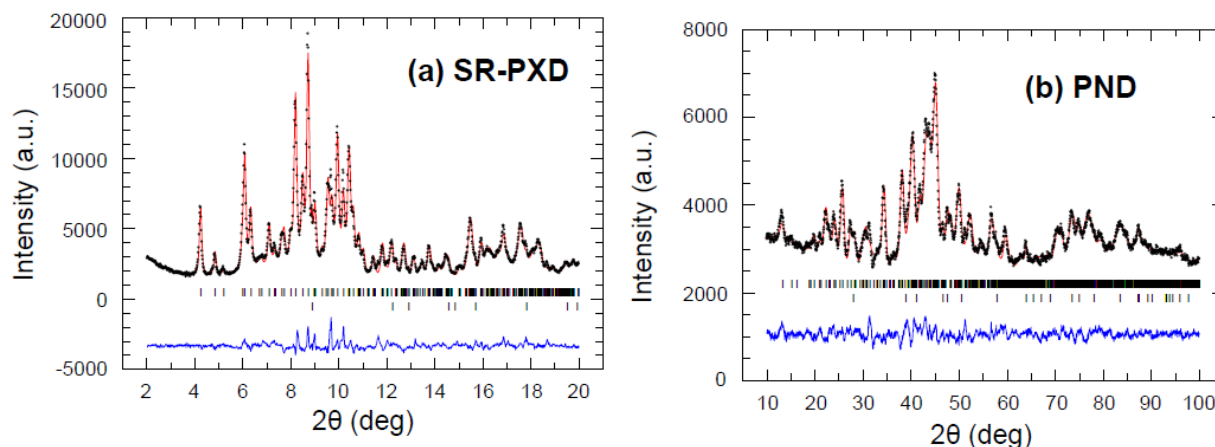


Figure 3 Rietveld fits of $\text{Ca}(\text{AlD}_4)_2$ to a) SR-PXD data and b) PND data. Upper and lower tick marks show Bragg peaks from $\text{Ca}(\text{AlD}_4)_2$ solid solution and AlD_3 , respectively.

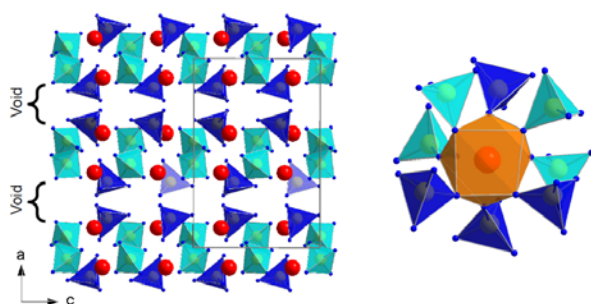


Figure 4 The crystal structure of $\text{Ca}(\text{AlD}_4)_2$ (left). The coordination of Ca is outlined (right)

Fluorine-substitution in Na_3AlD_6

Metal-substitution is widely used in intermetallic metal hydrides to alter the properties. Complex hydrides, on the other hand, show very limited possibilities for cation substitution. However, we have found that fluoride anions can substitute hydrogen anions in Na_3AlH_6 . The anion-substituted phase was produced by hydrogenating a mixture NaF and Al catalysed with TiF_3 .

The product was characterized by high-resolution SR-PXD at BM01B and PND with the PUS diffractometer. The data show that a phase which is isostructural to Na_3AlD_6 and Na_3AlF_6 was formed. Due to the excellent scattering contrast between D and F with X-rays and the visibility of D for the neutrons, the structure and composition, $\text{Na}_3\text{AlD}_{1.95}\text{F}_{4.05}$ could be reliably refined. There is no indication of long-range ordering between the F and D. Quantitative phase analysis showed that the sample contained about 33w% of the anion-substituted alane.

PCT measurement has shown that the anion-substitution has a pronounced destabilizing effect compared to pure Na_3AlD_6 .

The results are published in Journal of Physical Chemistry C [3].

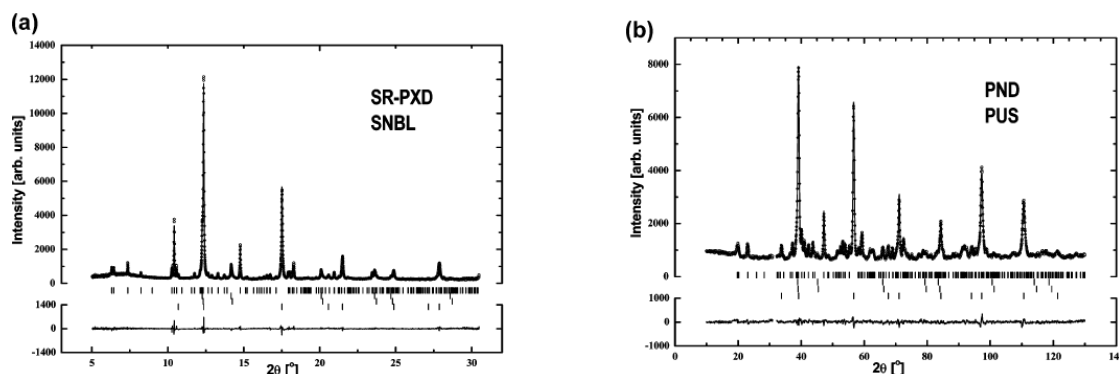


Figure 5 Rietveld fits of to a) SR-PXD data and b) PND data. Tick marks from top to bottom show Bragg peaks from $\text{Na}_3\text{AlD}_{6-x}\text{F}_x$, Al, $\text{Al}_{1-x}\text{Ti}_x$ and NaF.

CaB_2H_2 - an intermediate decomposition product from $\text{Ca}(\text{BH}_4)_2$

$\text{Ca}(\text{BH}_4)_2$ is considered as an attractive hydrogen storage material due to high gravimetric capacity and expected thermodynamic properties suitable for mobile hydrogen storage applications. However, the decomposition route of this compound is unclear and appears to be highly dependent on the experimental conditions.

In samples partly decomposed in our home laboratory “Temperature Programmed Desorption” (TPD) set-up, we have observed formation of an intermediate phase which is not observed in our recent in-situ SR-PXD measurements [4]. The phase appears during the first decomposition step of $\text{Ca}(\text{BH}_4)_2$. A sample which was rich in this intermediate phase, was produced by stopping the TPD right after the first desorption step (370 °C) and quickly cool to room temperature. The sample was measured with high-resolution SR-PXD at BM01B and the data could be indexed according to the orthorhombic unit cell $a = 12.81 \text{ \AA}$, $b = 4.08 \text{ \AA}$, $c = 3.90 \text{ \AA}$. The extinction rules pointed to the space groups $Pnna$ or $Pbna$. However, no structure solution succeeded in these space groups. Due to the high number of possible space groups with less systematic abscent, a search for isostructural phases with similar unit cell and reasonable stoichiometry was performed in the ICSD database. A model based on the HgCl_2 -type structure (space group $Pnma$) yielded a superior fit to the experimental data compared to all other evaluated structure types.

Rietveld refinement of the with Ca and B alone (substituted for Hg and Cl, respectively) yielded a satisfactory fit to the SR-PXD data. Two hydrogen positions were located by Difference Fourier Mapping, indicating a total composition CaB_2H_2 .

The structure model is shown in Figure 7. It consists of layers Ca atoms which are separated by alternating B layers and layers with infinite BH_2 -chains. The chains consist of direct -B-H-B-H- links with a terminal H on each boron atom. This is a structural feature which is not reported in any other B-H containing phases and should thus be confirmed with neutron diffraction. However, do to the strong absorption in natural boron and incoherent scattering from natural hydrogen, a double isotope substituted sample, $\text{Ca}^{11}\text{B}_2\text{D}_2$ sample must be prepared.

In a preliminary attempt to make $\text{Ca}^{11}\text{B}_2\text{D}_2$, $\text{Ca}^{11}\text{BD}_4$ was decomposed at lower temperature (320°C) and under a deuterium back-pressure to compensate for the lower stability of the deuteride. SR-PXD of the product reveals no $\text{Ca}^{11}\text{B}_2\text{D}_2$, but rather a mixture of α - and β $\text{Ca}(\text{BD}_4)_2$, CaD_2 and new, unidentified phase (Figure 8).. The efforts to prepare $\text{Ca}^{11}\text{B}_2\text{D}_2$ and to identify the new decomposition product are in progress.

The results are published in Journal of Materials Chemistry [5]

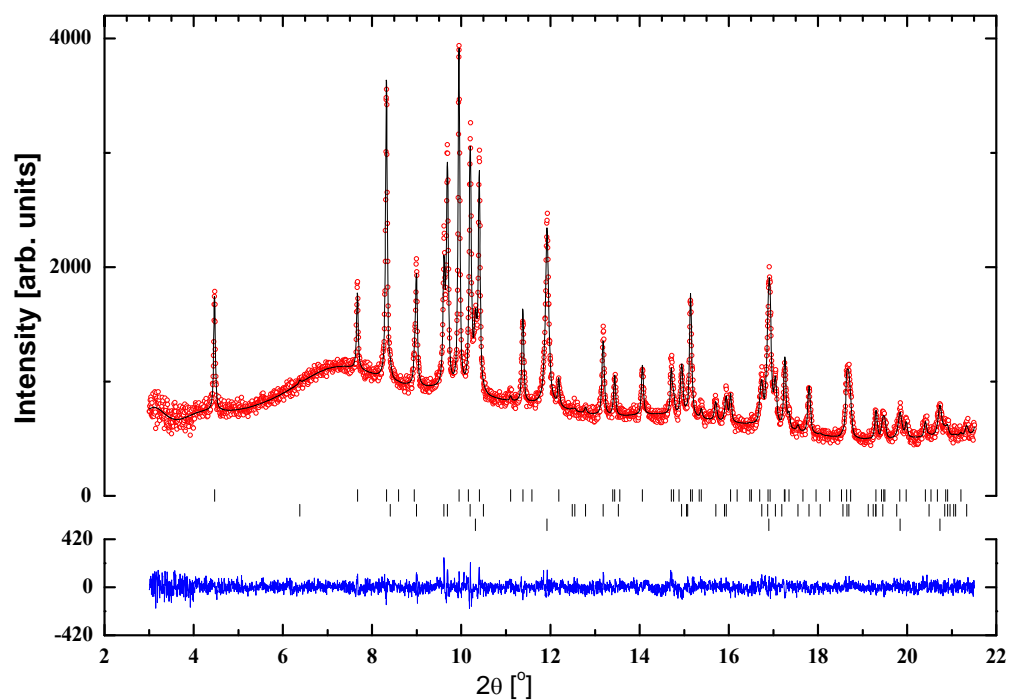


Figure 6 Rietveld fit for the CaB₂ sublattice of the proposed CaB₂H_x-phase showing observed. The positions of Bragg reflections are shown from CaB₂H_x (upper), CaH₂ (middle) and CaO (lower).

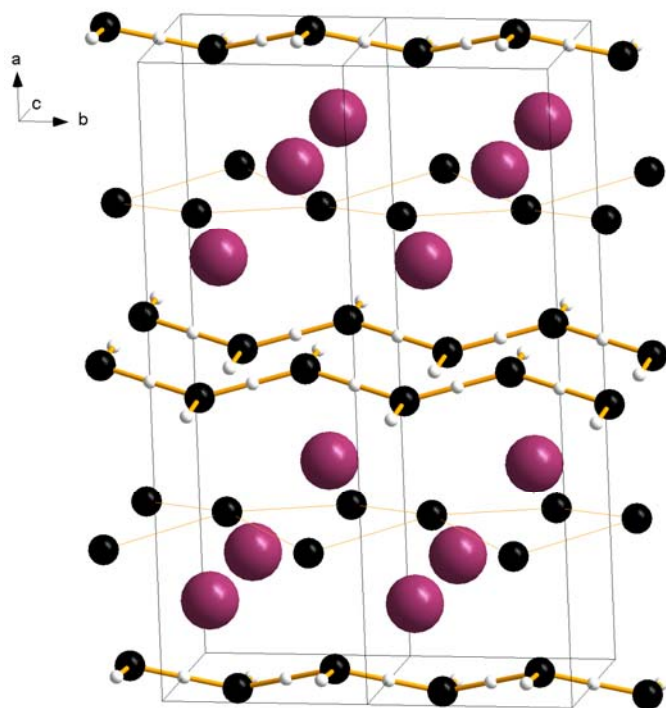


Figure 7 Proposed crystal structure of CaB₂H₂.

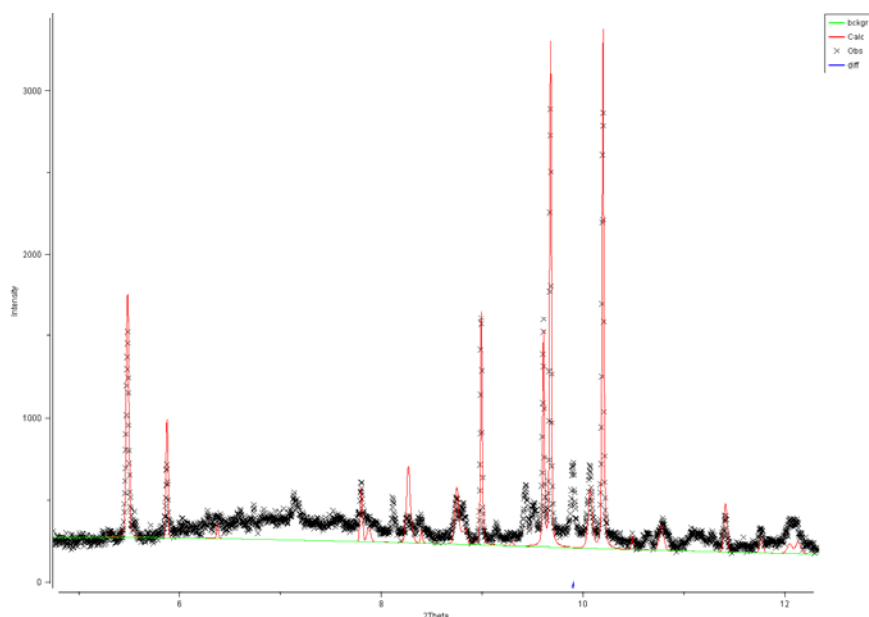


Figure 8 SR-PXD data for partly decomposed $\text{Ca}({}^{11}\text{BD}_4)_2$. The fitted peaks are from α - and β - $\text{Ca}({}^{11}\text{BD}_4)_2$. The unfitted peaks are from an unidentified phase.

Rehydrogenation of CaB_2H_x

The dehydrogenated powder containing the intermediate CaB_2H_x -phase (see above) was rehydrogenated at 306 °C and 96 bar. The starting material, the dehydrogenated powder and the rehydrogenated powder were studied by SR-PXD, and the data show reversibility of the intermediate phase under these relatively mild conditions.

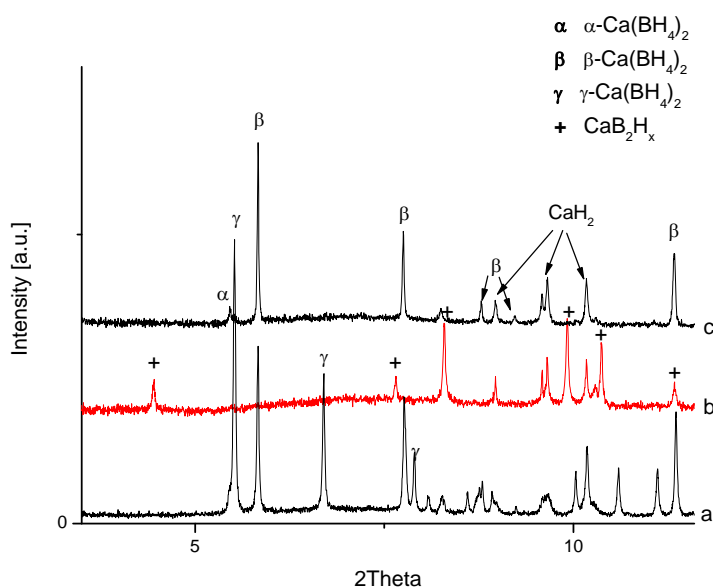


Figure 9 SR-PXD data for as-synthesized $\text{Ca}(\text{BH}_4)_2$ (a), dehydrogenated powder containing the intermediate CaB_2H_x -phase and CaH_2 (b) and rehydrogenated powder containing $\text{Ca}(\text{BH}_4)_2$ and CaH_2

A communication of these results for Journal of Materials Chemistry is in the final stage of preparation.

The crystal structure of $\text{LiSc}(\text{BH}_4)_4$

A new mixed borohydrides, $\text{LiSc}(\text{BH}_4)_3$ was synthesized at Hawaii University. Lab-PXD data revealed a highly crystalline product with no resemblance to any phases in the PDF-4. The data could be indexed according to a cubic unit cell with $a = 6.08 \text{ \AA}$. However, the superior resolution at BM01B revealed a slight but significant peak splitting, indicating lower symmetry (see inset in Figure 10). The pattern was successfully indexed with a pseudo-cubic tetragonal unit cell, $a = 6.076 \text{ \AA}$ and $c = 12.034 \text{ \AA}$. The crystal structure was solved and refined in space group $P-42c$ (Figure 10)

The structure consist of a $\text{Sc}(\text{BH}_4)_4^-$ complex anions with tetrahedral coordination of 4 BH_4 around Sc. The Li ions where found to be highly disordered and the Li position had to be splitt in two half-occupied positions to get a good agreement with SR-PXD data in the Rietveld refinement (Figure 11). It is suspected that the disorder is dynamic and thus that $\text{LiSc}(\text{BH}_4)_4$ is a Li-ion conductor.

The results are published in The Journal of Physical Chemistry A [6].

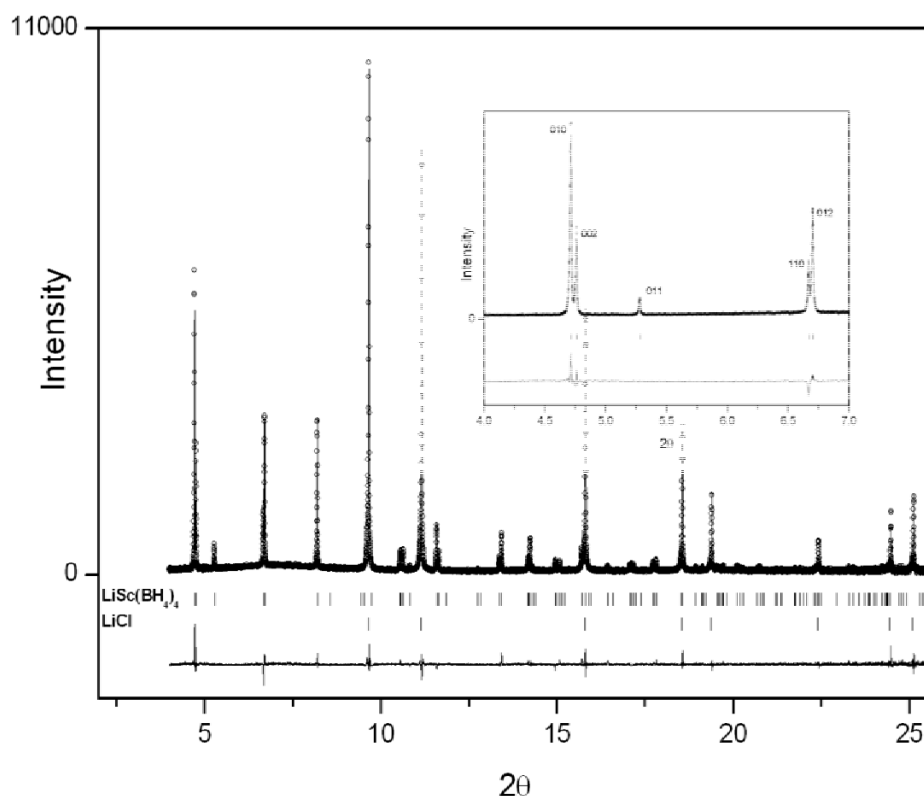


Figure 10 Rietveld fit of $\text{LiSc}(\text{BH}_4)_4$ to SR-PXD data. The subtle peak splitting due to pseudo-cubic unit cell is shown inset.

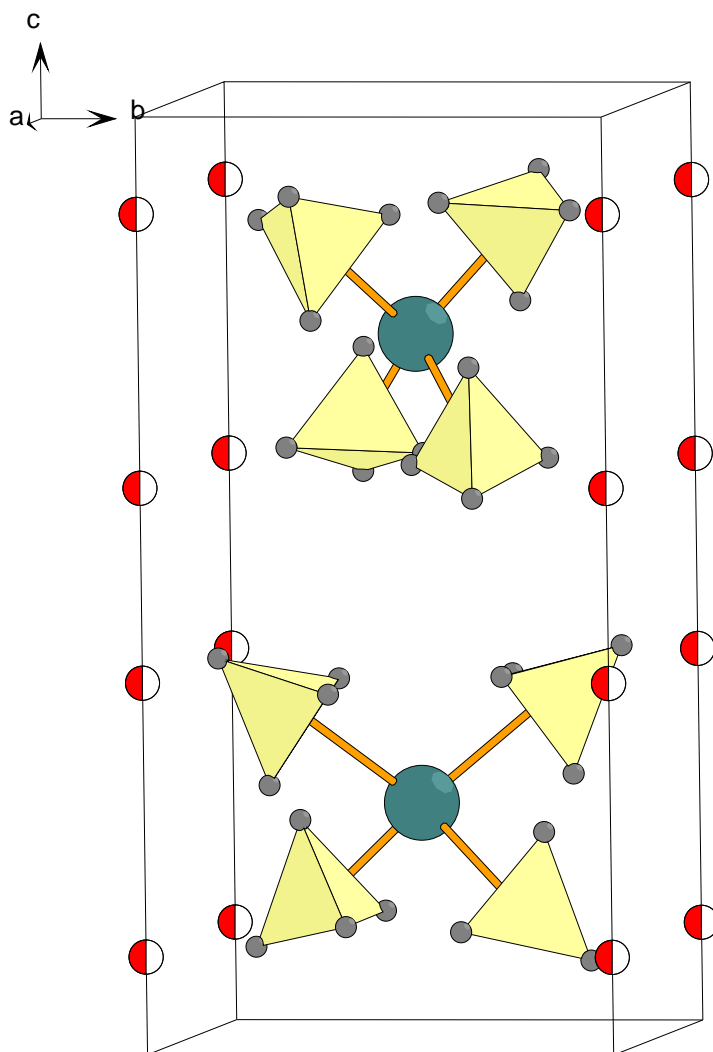


Figure 11 Refined structure of $\text{LiSc}(\text{BH}_4)_4$. Large green balls – Sc, tetrahedra – BH_4 , red and white balls – half-occupied Li sites.

Crystal structure of $\text{Mg}_2(\text{Fe}_{0.5}\text{Co}_{0.5})\text{D}_{5.5}$

Magnesium hydride, MgH_2 , has an attractive gravimetric hydrogen content of 7.6 w%H, but is too stable for most hydrogen storage purposes. Magnesium-based transition-metal complex hydrides, e.g. Mg_2NiH_4 , Mg_2FeH_6 and Mg_2CoH_5 , have more favourable thermodynamics at the expense of lower gravimetric hydrogen content (3.6-5.5 w%H in the given examples). The volumetric hydrogen density is superb. Mg_2FeH_5 contains 150 g_H/liter, which is the highest density in known hydrogen storage materials.

A mixed complex hydride, $\text{Mg}_2(\text{Fe}_{0.5}\text{Co}_{0.5})\text{D}_{5.5}$, was prepared by ball milling a 1:1 mixture of Mg_2FeD_6 and Mg_2CoD_5 . A homogeneous cubic face, isostructural to Mg_2FeH_6 , was confirmed by SR-PXD at BM01B. No traces of tetragonal Mg_2CoH_5 were detected, but small amounts of FeCo solid solution were present.

The crystal structure was refined with the SR-PXD data and PND data from PUS (JEEPII) (Figure 12). The structure is very similar to Mg_2FeD_6 and the high-temperature phase of Mg_2CoD_5 which constitute fcc packing of FeD_6 octahedra and CoD_5 square pyramids (randomly oriented), respectively. Mg is found in all tetrahedral interstices. The transition metals are randomly distributed over the fcc sites in $\text{Mg}_2(\text{Fe}_{0.5}\text{Co}_{0.5})\text{D}_{5.5}$. The coordination of the fcc site was refined as an octahedron with $5/6^{\text{th}}$ of a deuterium atom in each corner. This is

interpreted as a random distribution of FeD_6 octahedra and CoD_5 square pyramids since the square pyramid is essentially an octahedron with one missing corner. As in the high-temperature phase of Mg_2CoD_5 , there are no long-range correlations in the orientation of the square pyramids.

The results are published in Nanotechnology [7].

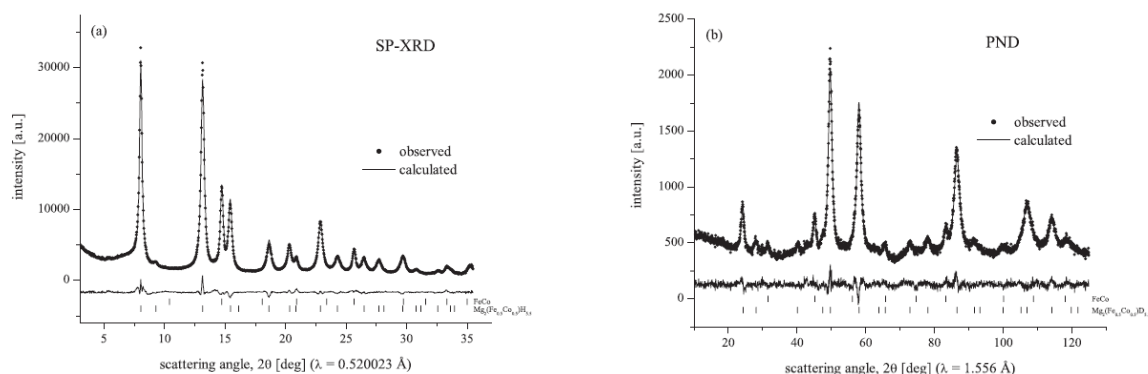


Figure 12 Rietveld fits of $\text{Mg}(\text{Fe}_{0.5}\text{Co}_{0.5})\text{D}_{5.5}$ to a) SR-PXD data and b) PND data. Upper and lower tick marks show Bragg peaks from FeCo solid solution and $\text{Mg}(\text{Fe}_{0.5}\text{Co}_{0.5})\text{D}_{5.5}$, respectively.

Hydride formation in Mg-based ternary systems

Mechanically activated Mg-based ternary systems are being investigated and their hydrogen sorption properties are explored. In particular, 4 Mg-Ti-Al samples were measured during the March 2009 experiment at MB01B.

Ball milling in H_2 produces a composite consisting of MgH_2 , TiH_2 and Al_3Ti . For this sample, decomposition of MgH_2 is observed at relatively low temperatures, around 240 °C. Ball milling in Ar of a powder mixture with the same composition results in the formation of a Mg/ Al_3Ti composite. In this case, the hydrogen sorption occurs with a more sluggish kinetics and at higher temperatures.

Preliminary results from SR-PXD at BM01B suggest that the Al_3Ti is in fact a mixture of an fcc Al-Ti solid solution and L12 Al_3Ti (see Figure 13). The relative amounts of such phases, which depend on the thermal history of the sample, are being evaluated at the moment. The aim is to identify which Al-Ti phase might have a beneficial effect on the hydrogen sorption properties of Mg/ MgH_2 .

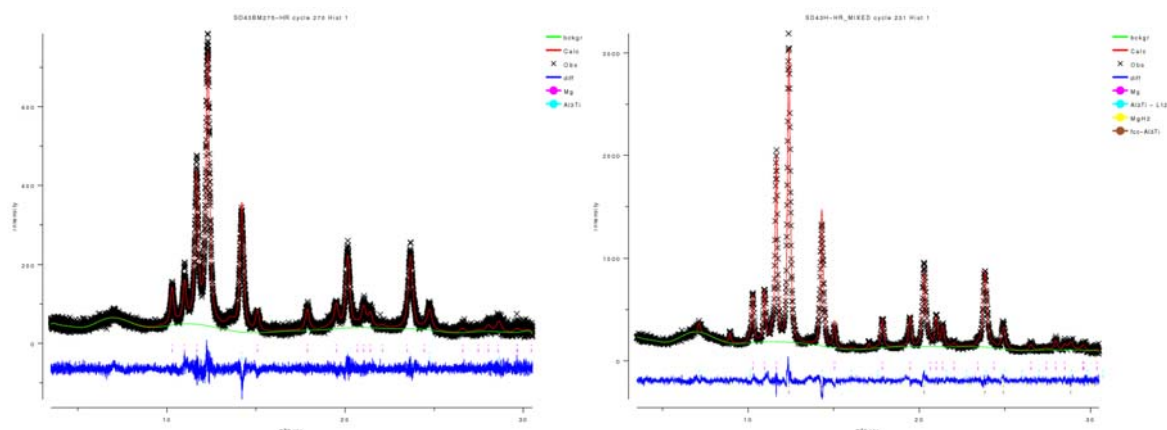


Figure 13 High-Resolution SR-PXD of $(\text{Mg}_{0.8}\text{Ti}_{0.2})_2\text{Al}$ after ball milling in Ar (left) and after ball-milling in Ar and annealing in H_2 at 330 °C and 30 bar (right).

Li₂ND

Li₂NH (lithium imide) is an intermediate product in several reactions considered for hydrogen storage. Its crystal structure is not unambiguously determined. The most thorough investigation was performed by Balogh et al by SR-PXD and PND on a deuterated sample, Li₂ND. They found 3 structure models, one disordered cubic ($a \sim 10$ Å) and two ordered orthorhombic (pseudo-cubic), which described the experimental data equally well. Above ca. 90°C, the phase took a (more) disordered face-centered cubic structure ($a \sim 5$ Å).

A double isotope substituted lithium imide sample, ⁷Li₂ND, was prepared to clarify the room-temperature structure. ⁷Li was used due to its far smaller absorption cross section for neutrons than natural Li. PND (PUS, JEEP II) show several weak peaks that are inconsistent with cubic symmetry.

SR-PXD measurements at BM01B were collected at room temperature and 100°C. The 100°C pattern could be indexed according a small cubic unit cell with unit cell axes of half of that suggested by Balogh et al ($a \sim 5$ Å). The RT pattern is noticeably different in two aspects: 1) there are additional peaks and 2) the cubic peaks are split into multiplets. The first point indicates an enlargement of the unit cell and the second point indicates lattice deformation. None of the unit cells suggested previously are consistent with the present data.

Supplementary PND data from PUS show the same additional peaks, but with higher relative intensity as the SR-PXD data. Structure determination is in progress.

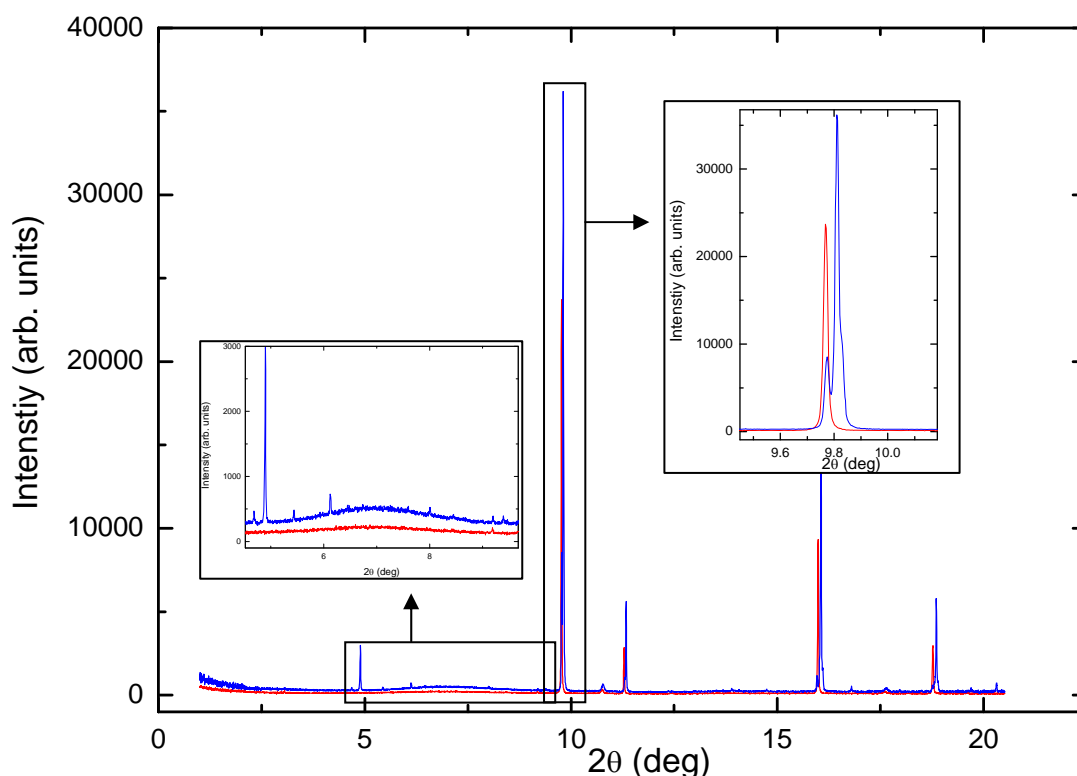


Figure 14 SR-PXD data for ⁷Li₂ND at RT (blue) and 100°C (red). Insets show ordering reflections (left) and peak splitting (right) at RT.

LiBH₄ in carbon aerogel

Preparation of LiBH₄ as nanoscopic particles is a possible route to lower the hydrogen desorption temperature.

LiBH₄ embedded in a carbon aerogel with a nominal pore size of 25 Å was measured at BM01B. The Bragg peaks were severely broadened compared to bulk LiBH₄ (Figure 15). The particle size was estimated to 20.3(7) nm using Rietveld refinement the Scherrer formula. It was assume to be no peak broadening from strain.

The result is not yet published but is expected to be included in a later publications.

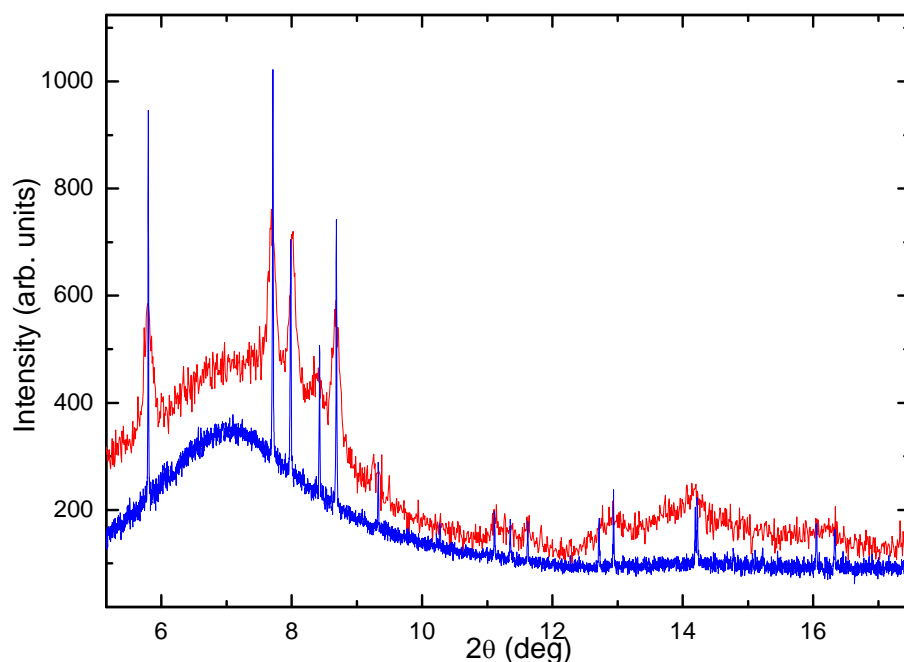


Figure 15 Bulk LiBH₄ (blue) and LiBH₄ embedded in a carbon aerogel (red).

Transition metal (TM)-aluminium phases in TM-enhanced NaAlH₄

An extensive investigation of performance and phase formation in TM-enhanced NaAlH₄ has been undertaken. The work is heavily based on SNBL beam time outside this long-term project, but since a significant amount of measurements were done with beam time from this project, it should be mentioned here.

A major result of the investigation concerns there whereabouts of the TM (typically Ti) after it is added to NaAlH₄, since no crystalline TM-containing phases are observed by diffraction. Careful examination of high-resolution SR-PXD data of NaAlH₄ treated with different TM-salts, show amorphous halos which can be assigned to amorphous TM-Al phases (Figure 16). The observations have been backed up by high-resolution TEM.

A small part of the results are published in Acta Materialia [8] but a series of five papers presenting the bulk of the results, are under preparation and will be submitted to Phys. Rev. B.

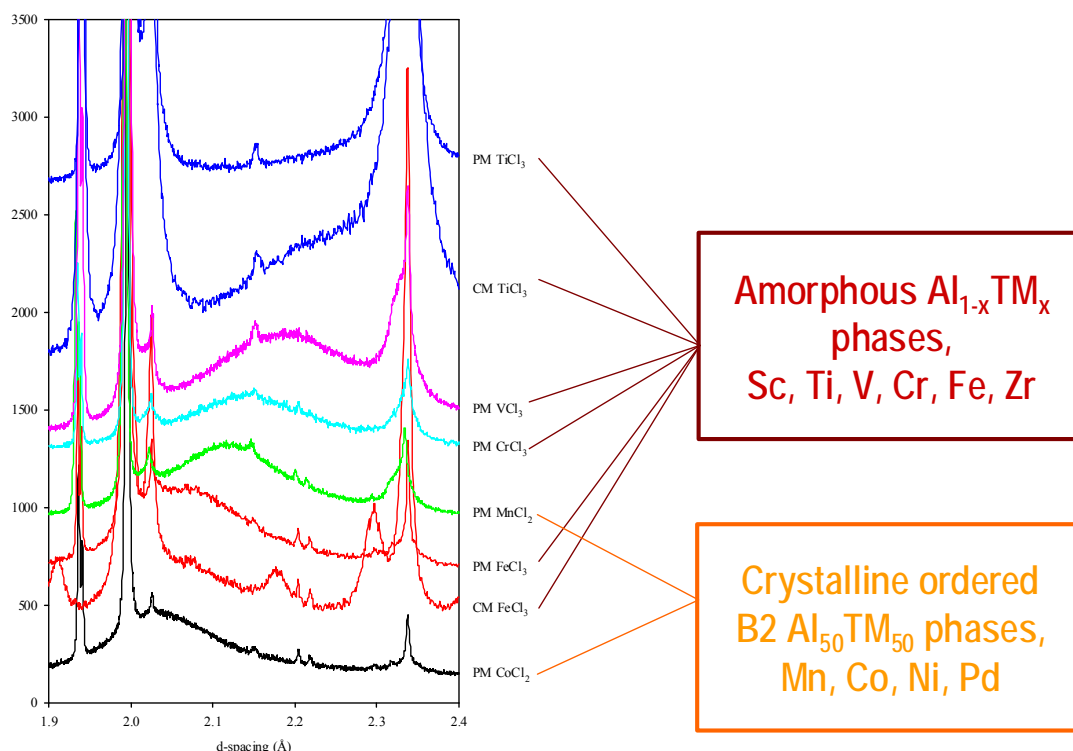


Figure 16 High-resolution SR-PXD data of NaAlH_4 with different TM-chloride additives. Note the diffuse halos from amorphous TM-Al-phases.

References to publications from long-term project 01-01-745

- [1] Grove, H.; Brinks, H.W.; Heyn, R.H.; Wu, F.J.; Opalka, S.M.; Tang, X.; Laube, B.L.; Hauback, B.C.: The structure of $\text{LiMg(AlD}_4\text{)}(3)$. *J. Alloys Comp.* **455** (2008) 249-254
- [2] Grove, H.; Brinks, H.W.; Lovvik, O.M.; Heyn, R.H.; Hauback, B.C.: The crystal structure of LiMgAlD_6 from combined neutron and synchrotron X-ray powder diffraction. *J. Alloys Comp.* **460** (2008) 64-68
- [3] Brinks, H.W.; Fossdal, A.; Hauback, B.C.: Adjustment of the stability of complex hydrides by anion substitution. *Journal of Physical Chemistry C* **112** (2008) 5658-5661
- [4] Riktor, M.D.; Sørby, M.H.; Chlopek, K.; Fichtner, M.; Buchter, F.; Züttel, A.; Hauback, B.C.: In situ synchrotron diffraction studies of phase transitions and thermal decomposition of $\text{Mg(BH}_4\text{)}(2)$ and $\text{Ca(BH}_4\text{)}(2)$. *Journal of Materials Chemistry* **17** (2007) 4939-4942
- [5] Riktor, M.D.; Sørby, M.H.; Chlopek, K.; Fichtner, M.; Hauback, B.C.: The identification of an hitherto unknown intermediate phase CaB_2H_x from decomposition of $\text{Ca(BH}_4\text{)}_2$. *Journal of Materials Chemistry* DOI: **10.1039/B818127F** (2009)
- [6] Hagemann, H.; Longhini, M.; Kaminski, J.W.; Wesolowski, T.A.; Cerny, R.; Penin, N.; Sørby, M.H.; Hauback, B.C.; Severa, G.; Jensen, C.M.: $\text{LiSc(BH}_4\text{)}(4)$: A novel salt of Li^+ and discrete $\text{Sc(BH}_4\text{)}(4)^{-}$ complex anions. *Journal of Physical Chemistry A* **112** (2008) 7551-7555
- [7] Deledda, S.; Hauback, B.C.: Formation mechanism and structural characterization of the mixed transition-metal complex hydride $\text{Mg}_2(\text{FeH}_6)_{0.5}(\text{CoH}_5)_{0.5}$ obtained by reactive milling. *Nanotechnology* **20** (2009) 204010
- [8] Pitt, M.P.; Vullum, P.E.; Sørby, M.H.; Sulic, M.P.; Jensen, C.M.; Walmsley, J.C.; Holmestad, R.; Hauback, B.C.: Structural properties of the nanoscopic $\text{Al}_{85}\text{Ti}_{15}$ solid solution observed in the hydrogen-cycled $\text{NaAlH}_4+0.1\text{TiCl}_3$ system. *Acta Materialia* **56** (2008) 4691-4701